Supporting Information

A Naphthalimide Derivative based Fluorescent Probe for Selective Detection of Hydrogen Peroxide and H_2O_2 vapor

Lin E Guo,[a] Yu Qiang Zhao,[c] Jia Zhong Zhang *[a] and Ying Zhou [b]

[a] College of counter-terrorism, Yunnan Police College, Kunming 650223, China.

[b] College of Chemical Science and Technology, Yunnan University, Kunming 650091, China

[c] Yunnan Key Laboratory of Chiral Functional Substance Research and Application, School of Chemistry & Environment, Yunnan Minzu University, Kunming 650091, China.

Content

Experimental Section

1. Syntheses of NAPP

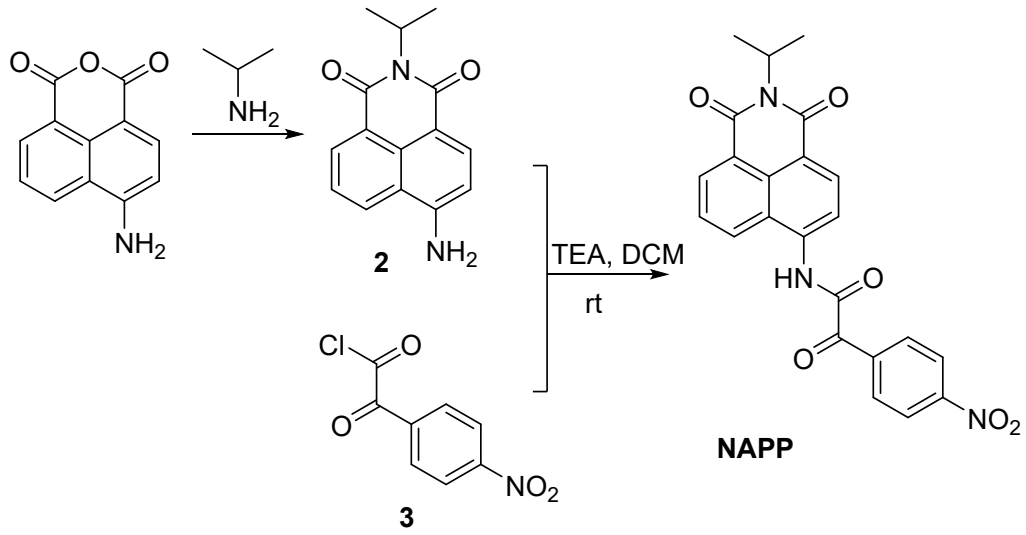

Scheme S1 Synthesis of **NAPP**

2. Optimizing conditions

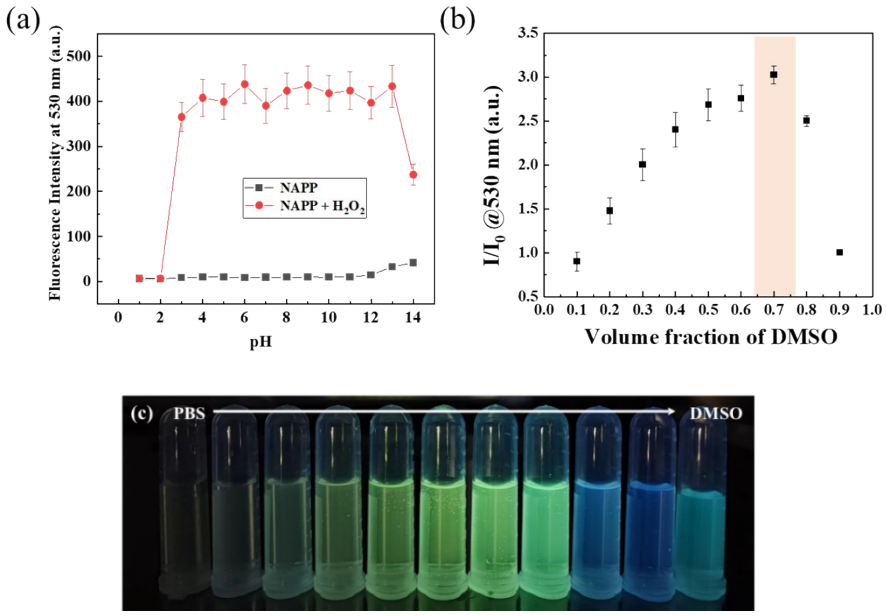

Fig. S1 (a) Fluorescence signals at 535 nm of **NAPP** and **NAPP** in the presence of H_2O_2 in DMSO·PBS (0.05 M, 7:3 v/v) buffer solutions of different pH; (b) fluorescence signals of **NAPP** at 530 nm before (I_0) and after (I) addition of H_2O_2 with different volume of DMSO, and (c) the color changes observed in the presence of H_2O_2 with different volume of DMSO. [**NAPP**] = 10 μM, [H_2O_2] = 100 mM, λ_{ex}= 433 nm.

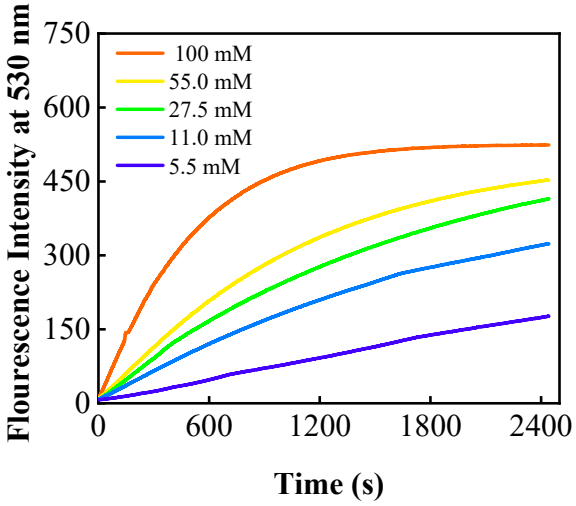

Fig. S2 Time tracking of **NAPP** with different concentrations (5.5 mM, 11 mM, 27.5 mM, 55 mM and 100 mM) of H_2O_2 in DMSO·PBS (50 mM, pH=7.4, 7:3 v/v) buffer solutions. [**NAPP**] = 10 μM, λ_{ex}= 433 nm.

3. Ultraviolet Absorption Spectrophotometric Titration

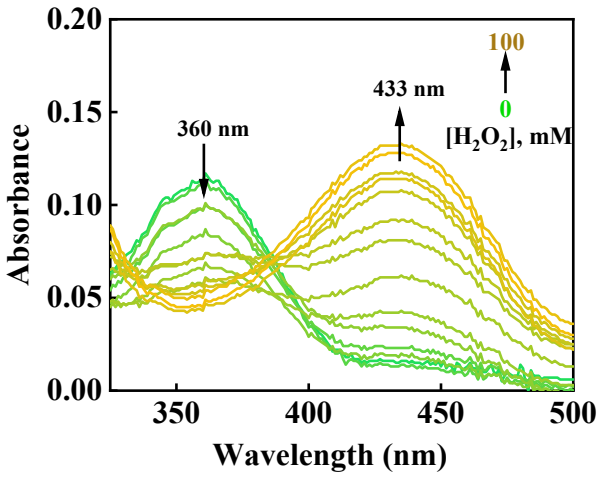

Fig. S3 Absorption titration spectra of **NAPP** (10 μM) in the presence of varying concentrations of H_2O_2 in 7:3 (v/v) DMSO·0.05 M pH 7.4 PBS buffer.

4. The apparent rate constant and pseudo-first-order rate constant

Table S1 Apparent rate constant (k_{obs}) of the reaction between **NAPP** (10 μM) and H_2O_2.

Concentrations of H_2O_2	**k_{obs}-means (s^{-1})**	**R^2**
100 mM	0.0423	0.992
55 mM	0.03016	0.990
27.5 mM	0.01988	0.991
11 mM	0.01383	0.978
5.5 mM	0.00381	0.964

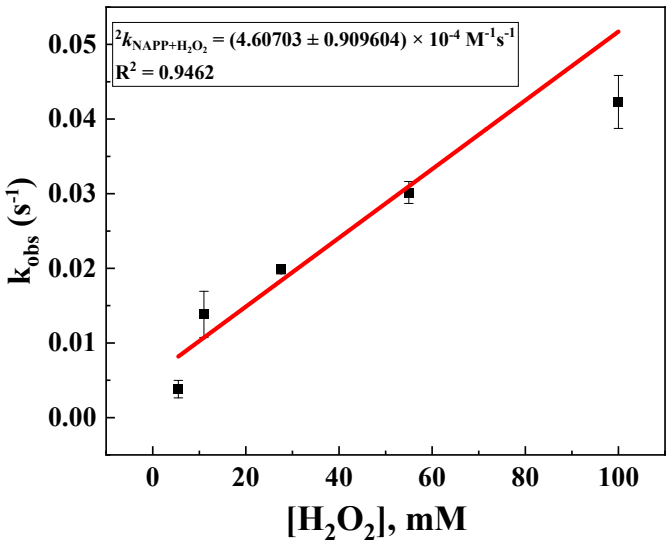

Fig. S4 The dependences of the second-order rate constant of the reaction between **NAPP** and H_2O_2 on the initial concentration of H_2O_2. Reaction mixtures contained 10 μM **NAPP**, 7:3 (v/v) DMSO·0.05 M PBS buffer (pH 7.4), 5.5-100 mM H_2O_2.

5. The linear range and detection limit

The detection limit was calculated based on the method reported in the previous literature [1]. The fluorescence emission spectrum of **NAPP** (5.0×10^{-6} M) was measured by twenty times and the standard deviation of blank measurement was achieved. The fluorescence intensity at 530 nm was plotted as a concentration of H_2O_2. The detection limit was calculated by using detection limit 3σ/k: Where σ is the standard deviation of blank measurement, k is the slope between the fluorescence intensity versus H_2O_2 concentration.

Table S2 Examples and structures of the known naphthalimide sensors and their detection limit.

Probe	Structures	Detection objects	Detection limit	Ref
α-Naph	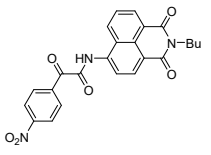	hydrogen peroxide	38 nM	[2]
MNG	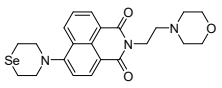	hydrogen peroxide	61 nM	[3]

NPB	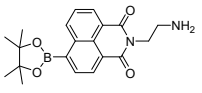	hydrogen peroxide	15 nM	[4]
NAPB	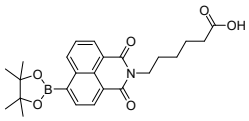	hydrogen peroxide	4.34 nM	[5]
TSY-1	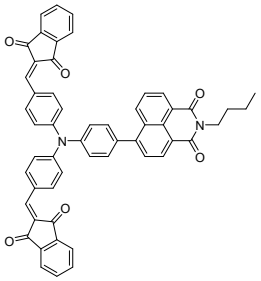	hydrazine	54 μM	[6]
This work	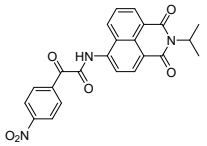	hydrogen peroxide	59.6 nM	—

6. Competition experiment

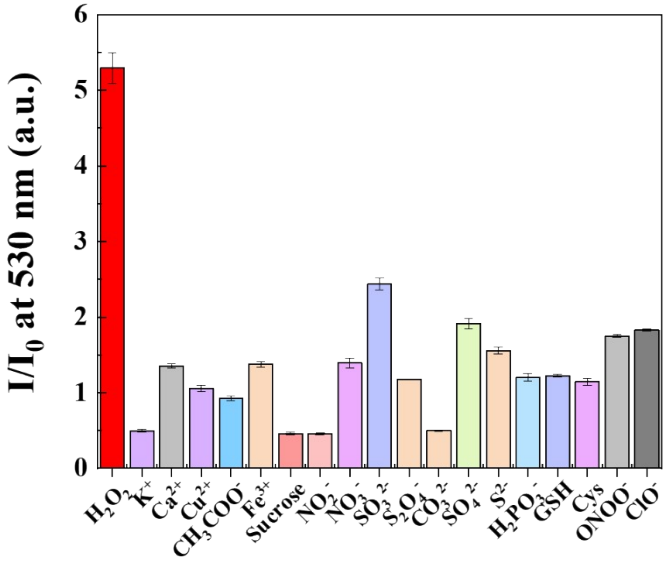

Fig. S5 Selectivity assay of fluorescence responses of the NAPP in the presence of 100 mM of $ONOO^-$, K^+, Ca^{2+}, Cu^{2+}, CH_3COO^-, Fe^{3+}, Sucrose, SO_3^{2-}, $S_2O_4^-$, CO_3^{2-}, SO_4^{2-}, S^{2-}, $H_2PO_3^-$. GSH and Cys in PBS (50 mM, pH=7.4, 7:3 v/v) buffer solutions. I_0 and I were the fluorescence intensities of

the **NAPP** at 530 nm without and with the addition of different species, respectively. [**NAPP**] = 10 μM.

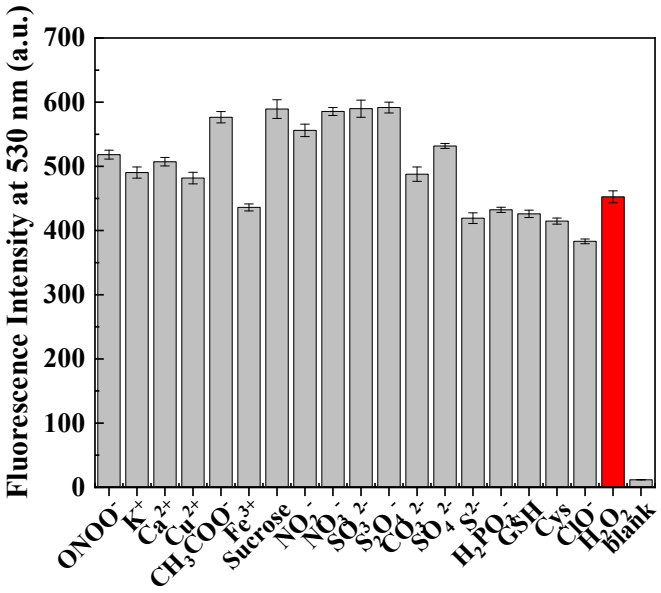

Fig. S6 Fluorescence intensity of **NAPP** and H_2O_2 in DMSO·PBS (50 mM, pH=7.4, 7:3 v/v) buffer solutions, with 100 mM of $ONOO^-$, K^+, Ca^{2+}, Cu^{2+}, CH_3COO^-, Fe^{3+}, Sucrose, SO_3^{2-}, $S_2O_4^-$, CO_3^{2-}, SO_4^{2-}, S^{2-}, $H_2PO_3^-$. GSH and Cys. [NAPP] = 10 μM, [H_2O_2] = 100, λex= 433 nm.

7. Job-plot experiment

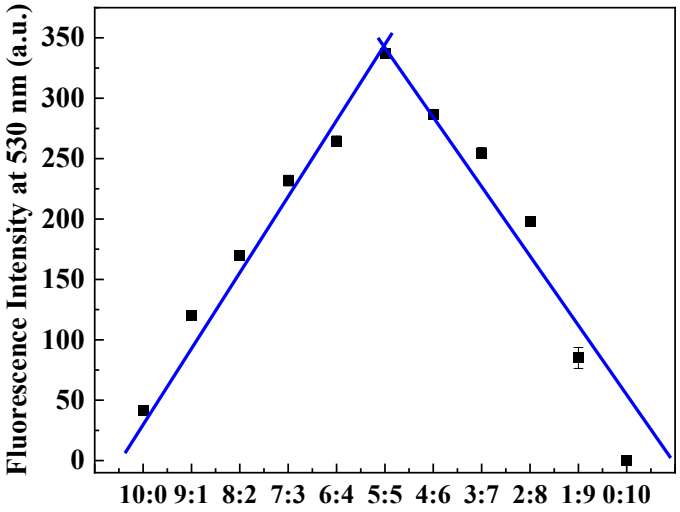

Fig. S7 The Job Plot using fluorescent intensity at 530 nm of **NAPP** and H_2O_2 in DMSO·PBS (50 mM, pH=7.4, 7:3 v/v) buffer solutions. The total concentration of **NAPP** and H_2O_2 was 0.5 mM.

8. Mass spectrum of the NAPP probe interaction with H_2O_2

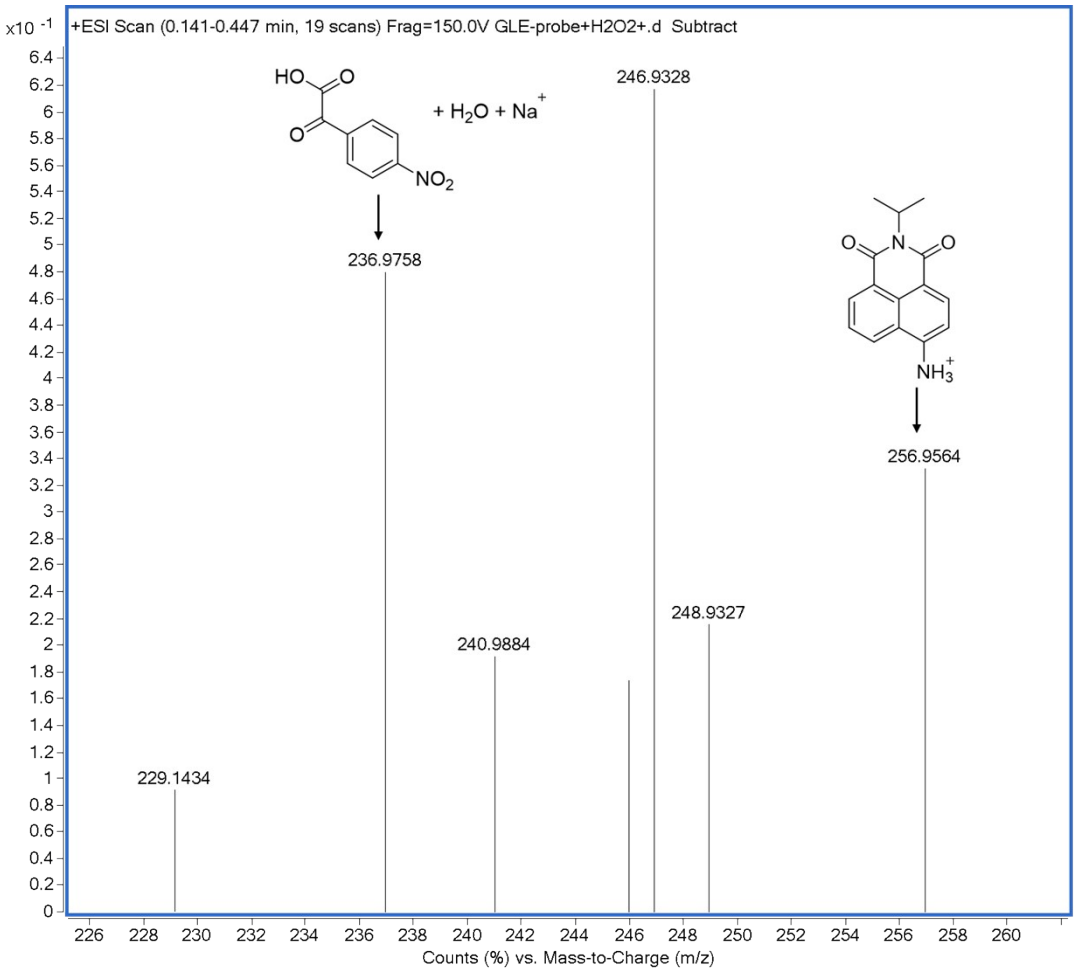

Fig. S8 Mass spectrum of compound **NAPP** in the prescence of H_2O_2

9. DFT calculation

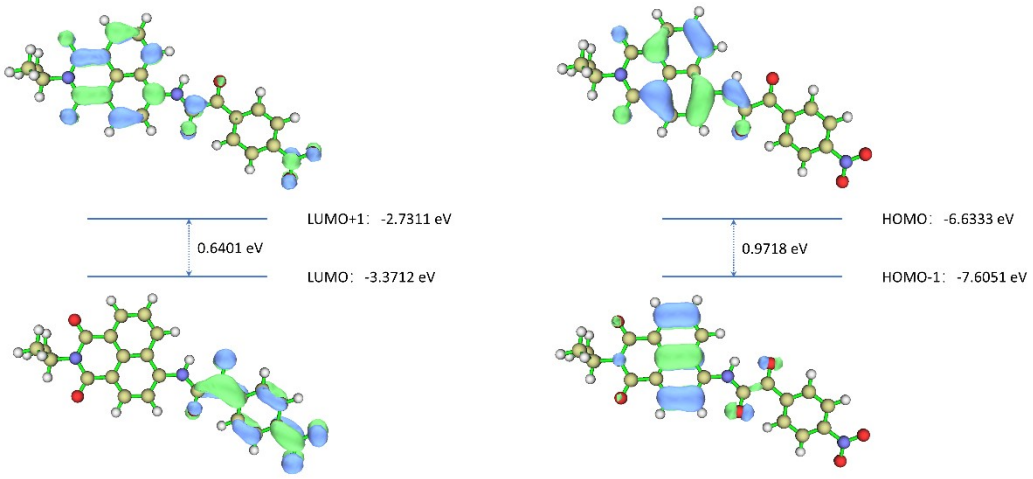

Fig. S9 Schematic representation of the orbital distribution of **NAPP** from HOMO-1 to LUMO+1 and the energy difference.

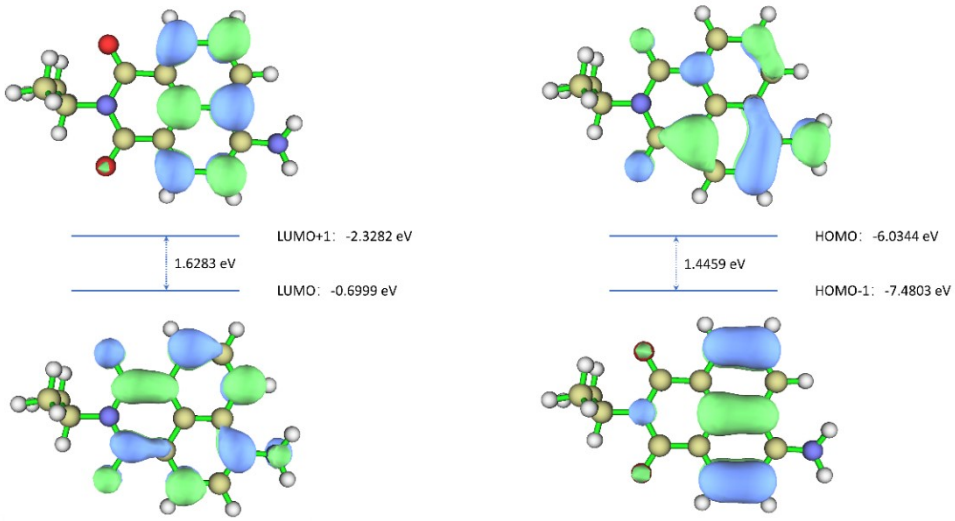

Fig. S10 Schematic representation of the orbital distribution of **NAP-NH_2** from HOMO-1 to LUMO+1 and the energy difference.

10. Fluorescence imaging of HepG2 cells

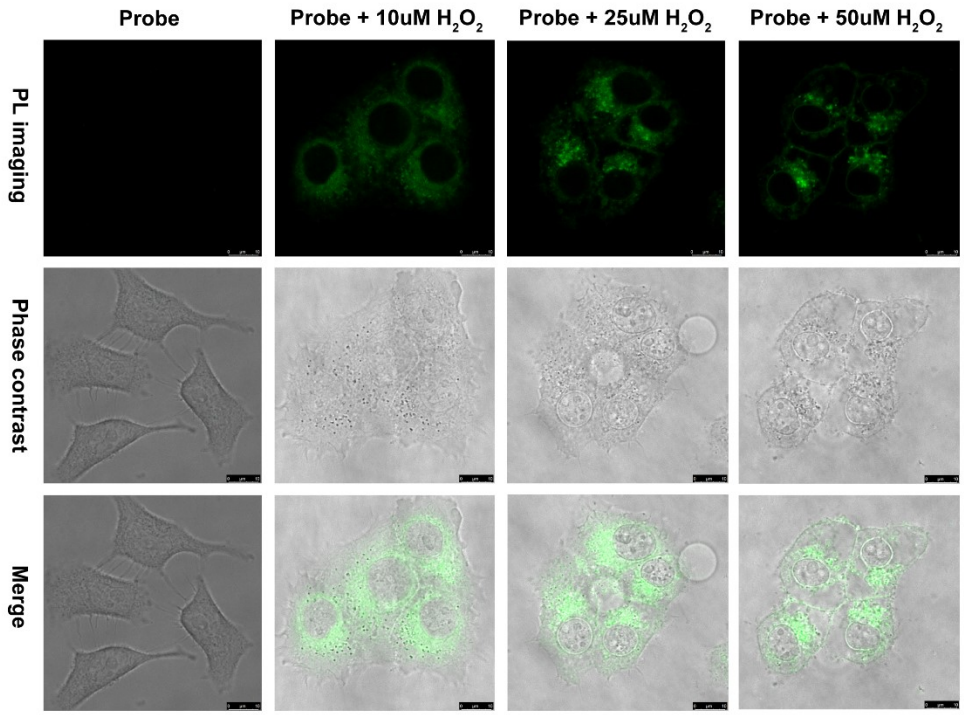

Fig. S11 Fluorescence imaging (top), phase contrast (middle), and merge (bottom) for HepG2 cells in different concentrations of H_2O_2 in vitro: a) with 10 μM probe only, b) with10 μM probe for 30 min and 10 μM H_2O_2 for 30 min, c) with10 μM probe for 30 min and 25 μM H_2O_2 for 30 min, c) with10 μM probe for 30 min and 50 μM H_2O_2 for 30 min. All images share the same scale bar (10 μm).

11. Compound characterization

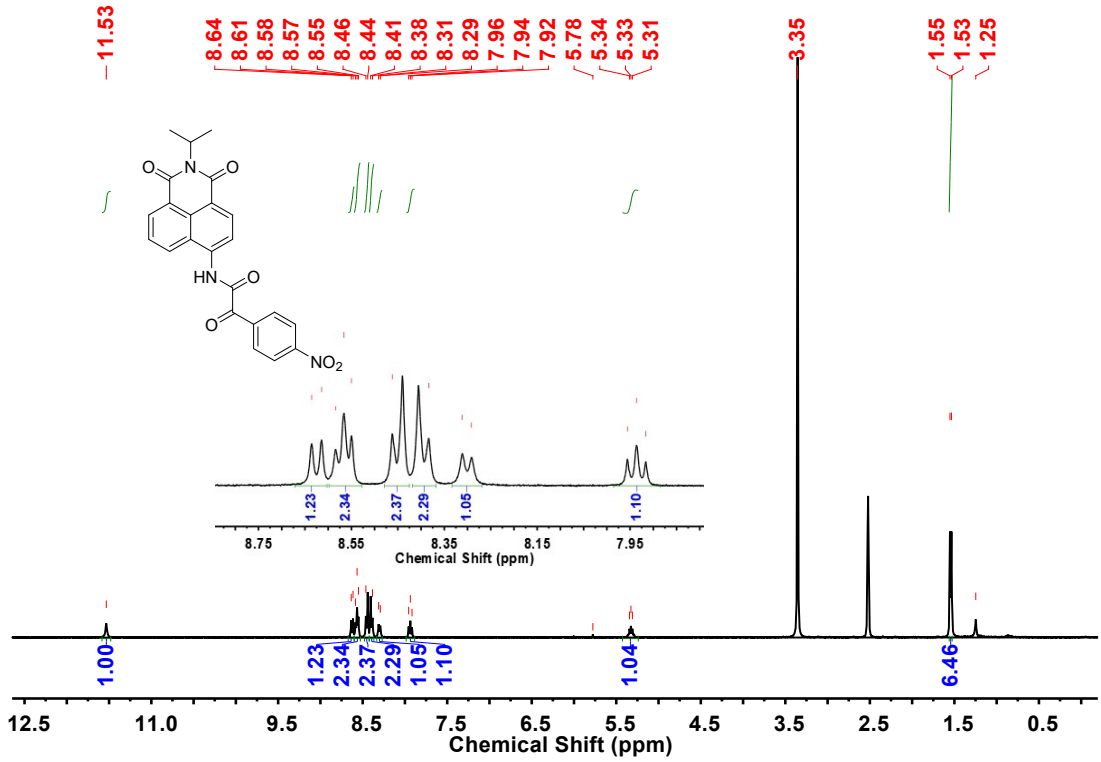

Fig. S12 ^{1}H NMR ($CDCl_3$, 500MHz) spectra of **NAPP**

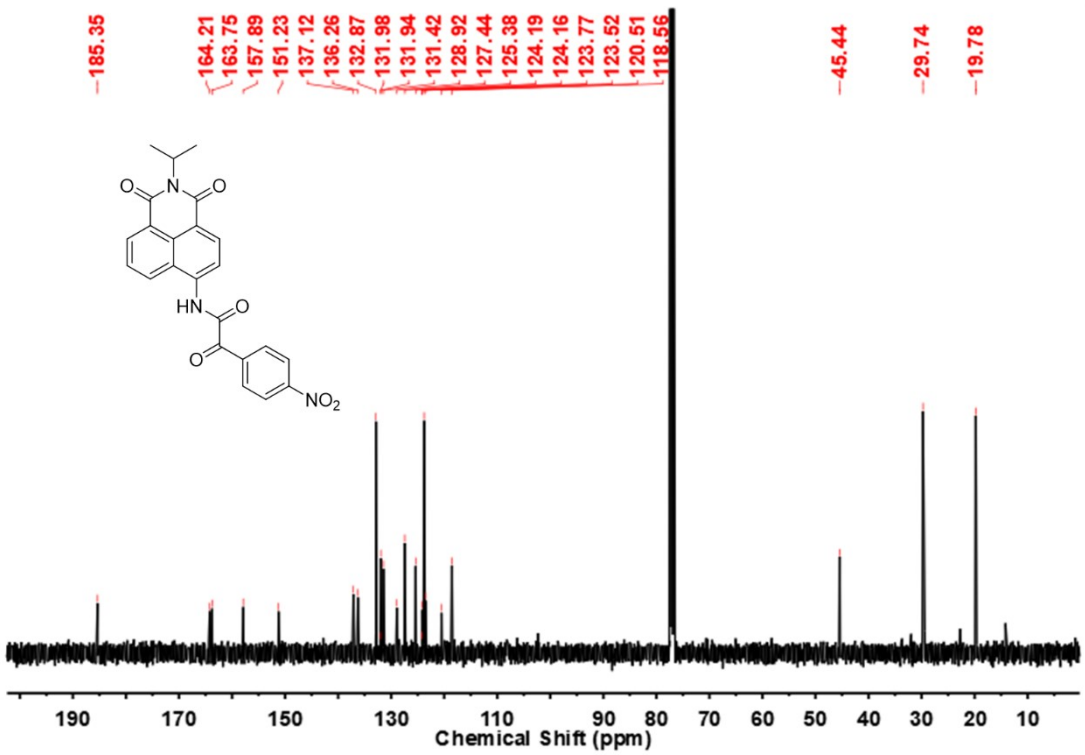

Fig. S13 ^{13}C NMR ($CDCl_3$, 125MHz) spectra of **NAPP**

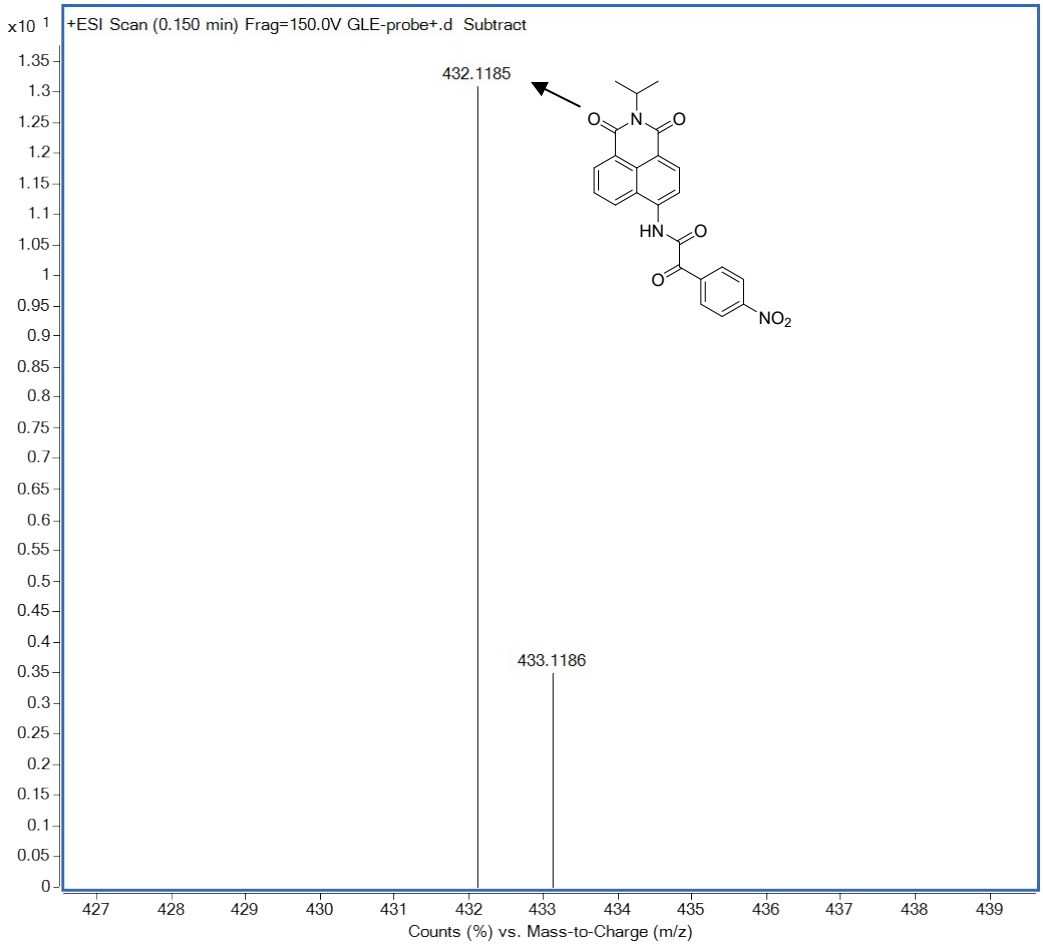

Fig. S14 FAB mass of compound **NAPP**

References

[1] B. Zhu, C. Gao, Y. Zhao, C. Liu, Y. Li, Q. Wei, Z. Ma, B. Du, X. Zhang, *Chem. Commun.,* **2011**, 47, 8656-8658.

[2] C. Gao, Y. Tian, R. Zhang, J. Jing, X. Zhang, *Anal. Chem.,* 2017, 89(23), 12945-12950.

[3] Y. Feng, D. Lei, B. Zu, J. Li, Y. Li, X. Dou, *Adv. Sci*., 2024, 11, 2309182.

[4] T. Ma, K. Fu, Z. Li, C. Yuan, W. Ma, *Spectrochim. Acta A*., 2022, 276, 121218.

[5] Z. Ding, X. He, J. Huang, R. Zhang, Y. Song, H. Yang, *ChemistrySelect* 2025, 10(5), e202405541.

[6] Z. Shang , S. Tian , Y. Wang , C. Zhang , Q. Meng , R. Zhang , Z. Zhang, *Sensor. Actuat. B. Chem*., 2024, 398, 134725.